OPEN

Phenothiazine Derivative-Accelerated Microbial Extracellular Electron Transfer in Bioelectrochemical System

Xian-Wei Liu[1], Xue-Fei Sun[2], Jie-Jie Chen[1], Yu-Xi Huang[1], Jia-Fang Xie[1], Wen-Wei Li[1], Guo-Ping Sheng[1], Yuan-Yuan Zhang[1], Feng Zhao[3], Rui Lu[1] & Han-Qing Yu[1]

[1]Department of Chemistry, University of Science & Technology of China, Hefei, 230026, China, [2]School of Environmental Science and Engineering, Shandong University, Jinan, 250100, China, [3]Institute of Urban Environment, Chinese Academy of Sciences, Xiamen, 361021, China.

In bioelectrochemical system (BES) the extracellular electron transfer (EET) from bacteria to anode electrode is recognized as a crucial step that governs the anodic reaction efficiency. Here, we report a novel approach to substantially enhance the microbial EET by immobilization of a small active phenothiazine derivative, methylene blue, on electrode surface. A comparison of the currents generated by *Shewanella oneidensis* MR-1 and its mutants as well as the electrochemical analytical results reveal that the accelerated EET was attributed to enhanced interactions between the bacterial outer-membrane cytochromes and the immobilized methylene blue. A further investigation into the process using *in situ* Raman spectro-electrochemical method coupled with density functional theory calculations demonstrates that the electron shuttling was achieved through the change of the molecule conformation of phenothiazine in the redox process. These results offer useful information for engineering BES.

In conventional waste treatment processes, not only substantial energy in organic matter is wasted but also extra energy should be invested[1]. Bioelectrochemical systems (BES) is recognized as an energy-saving alternative because it allows direct recovery of energy from waste streams like sewage[1,2]. From filling knowledge gaps in earth's biogeochemical cycles to powering different devices such as nano-sensors and detectors, BES offers a versatile platform for various technologies[3–6]. One common feature of all BES is a microbially catalyzed oxidation of substrate and subsequently transport of the generated electrons to the anode. However, the extracellular electron transfer (EET) from bacteria to anode electrode is usually a limiting step in this process and is recognized to be a crucial step in engineering BES[7]. In an effort to accelerate the anodic EET, one of the useful approaches is to use nanostructured chemical catalysts[8–10].

Three distinct EET pathways, i.e., through cell-surface proteins, mediator compounds (such as flavins), and cellular pili, also named nanowires, have been proposed in BESs. For some bacteria such as *Shewanella*, usually more than one type of EET pathways are involved[11–13]. These EET pathways inspire us in designing more powerful materials for BES in a biomimetic way. In our previous study, we fabricated a network-structured graphene oxide, which acted as nanowires to significantly enhance the anodic EET[14]. In addition, in light of a positive role of electron shuttles in EET but a unstable nature of these molecule in solution[12,15], immobilization of redox-active molecule on the electrode has also been adopted as an efficient way to promote microbial EET. For example, immobilization of 9,10-anthraquinone-2,6-disulfate on anode electrode using polyethyleneimine as a binder has been reported to improved microbial current generation[16]. However, one shortcoming of polyethyleneimine is the poor conductivity, which can to some extent limit the EET process. Furthermore, despite of intensive studies in the role of redox mediators in microbial reduction of electrodes, there has not been a conclusive consensus whether electrode modification with synthetic redox mediators could promote EET.

Phenazines are aromatic compounds with a dibenzo annulated azine structure. In their derivatives, a methyl and/or amino group is attached to the benzene rings, where one N can be substituted by S (phenothiazine) for example in the case of methylene blue (MB)[17]. These structures make them easy to be electropolymerized on electrode surface[18]. Like other electron shuttles, most phenothiazine derivatives have sufficiently-low reduction potentials ranging from -180 to 100 mV under usual physiological and environmental conditions. Thus, the redox reactions between reduced phenazines or thiazines and terminal electron acceptors are thermodynamically

feasible[19]. These features make them ideal candidates for electrode modification to enhance the microbial EET at BES anode.

Here, we attempt to accelerate anodic microbial EET in a BES by electropolymerization of small active phenothiazine derivatives on a carbon electrode. To achieve this, *Shewanella* was chosen as a model anodic microbe, and the anode electrode was electropolymerized with exogenous phenothiazine. The interactions between *Shewanella* and the as-prepared anode electrode were investigated by recoding the microbial current generation. In addition, the role of immobilized phenothiazine in EET was elucidated by coupling *in situ* Raman spectral-electrochemical analysis with density functional theory (DFT) to probe the conformation variations at a molecular level.

Results

Electron transfer at different potentials. Figure 1a shows the microbial current generated at a potential-poised electrode when an active phenothiazine of small molecules (either Toluidine blue O, Thionine, or MB) was used as the electron mediator. A BES without dosing any of the three phenothiazine derivatives was used as the control, which showed very low current density. A higher current density was produced with MB than with Toluidine blue O or Thionine. The current density peaked at 0.81 A/m² at the 10th hour for the MB-dosed BES, but only reached 0.65 and 0.21 A/m² for systems with Toluidine blue O and Thionine, respectively. By plotting the average of the peak current density of the three phenothiazine derivatives *vs.* their respective redox potential at the
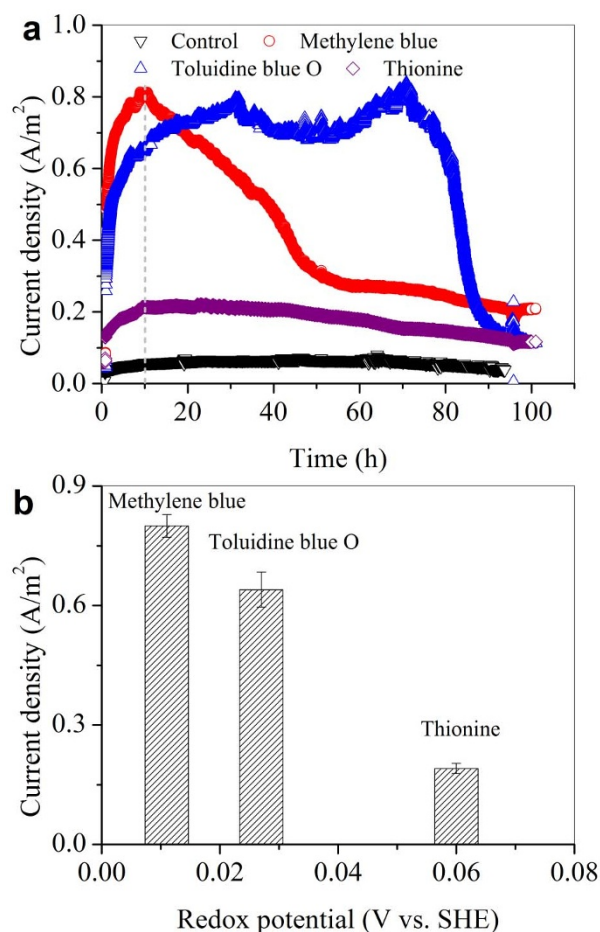
Figure 1 | Microbial EET recorded by the potential-poised electrodes in the presence of phenothiazine (a); plot of the maximum current densities of the three phenothiazine derivatives vs. their respective redox potentials (b).

10th hour (determined at pH 7.0 vs SHE; Figure 1b)[20], it was found that the phenothiazine derivatives with a lower redox potential tended to have a higher peak current density (Figure 1b). MB had a lowest redox potential of 0.011 V, and also possessed the largest peak current density among the three phenothiazine derivatives. Thus, in the sequential experiments, MB was chosen as the model phenothiazine derivative to modify the electrode.
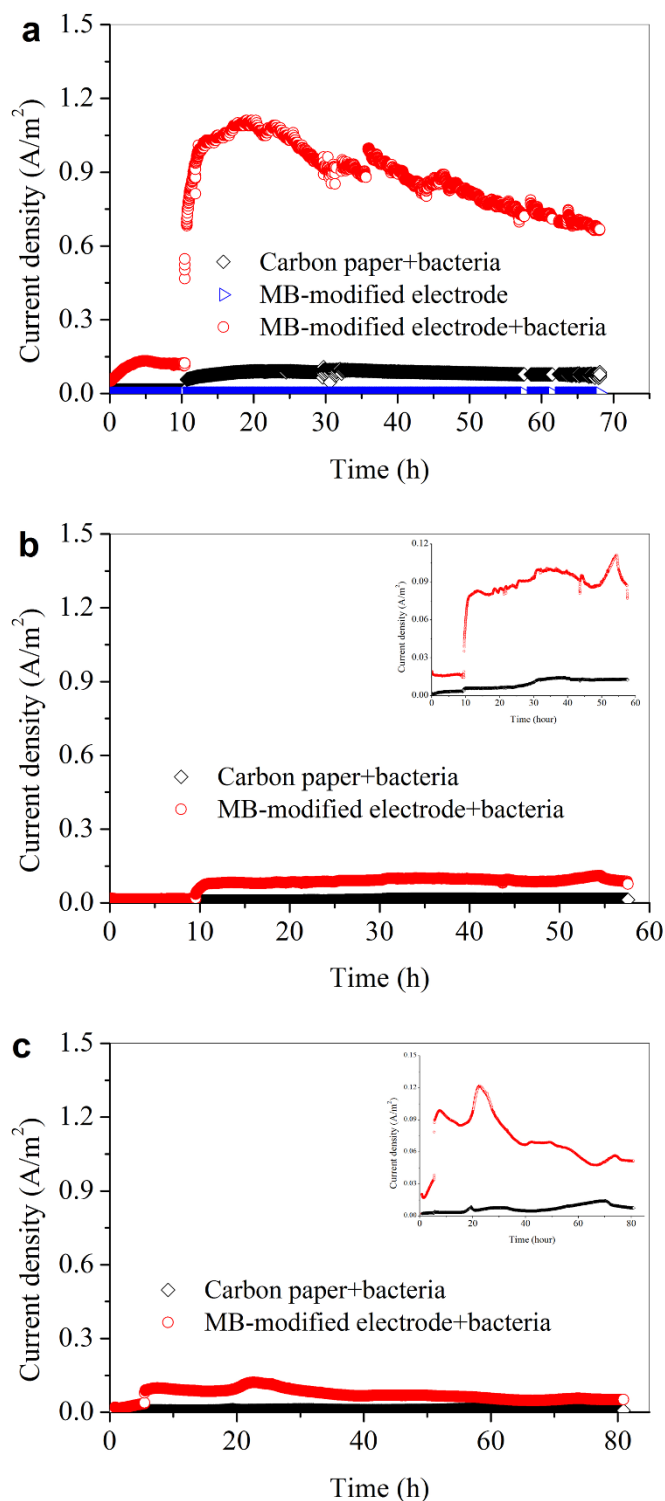
Enhanced microbial current generation by MB film. When a raw carbon paper was used as the control anode, the current density increased to 0.09 A/m² (Figure 2a). In comparison, with the MB-modified carbon paper, the current density drastically increased and peaked at 1.11 A/m², indicating a distinctive improvement in the microbial electron transfer (Figure 2a). To validate whether such a result was repeatable, each experiment was repeated. A similar current curve was obtained (Figure 2S). Notably, in our study only planar electrode was used, the modification of MB did not increase the available electrode surface area, and the electrode was poised at a relative low potential (0.1 V vs. Ag/AgCl) compared with the previous reports (from 0.12 to 0.2 V vs. Ag/AgCl; Table S1). Nevertheless, the obtained current density here was comparable to those with porous nano-structured electrodes reported in other studies (1.0–1.8 A/m²)[14,21].

It has been widely recognized that the *c*-type cytochromes in bacterial outer membrane play a significant role in direct electron transfer from cell surface to solid minerals or electrodes because of their unique location on cellular surface in the respiratory electron-transfer process. To investigate whether the interactions between MB and *c*-type cytochromes are responsible for the promoted electron transfer at the bacteria/electrode interface, *S. oneidensis* MR-1 mutants (*OmcA*/*MtrC*) were used. The current densities were 0.01 and 0.11 A/m² only for the control and the MB-modified electrodes, respectively (Figure 2b). Deletion of specific cytochromes significantly decreased the microbial current, indicating that both *MtrC* and *OmcA* played a key role in the electron transfer between the bacteria and MB interface. The experiment with mutant ΔMtrB further confirms the above results (Figure 2c).

It is well known that *S. oneidensis* MR-1 is able to excrete compounds such as flavins to shuttle electrons between cells and solid electron acceptor[12]. The CV results show that the BES with MB had a substantially lower redox current response to flavins than the control (Figure 3). The performance of the MB-modified electrode at different flavins concentrations in a range of 0–1.0 μM was further evaluated (Figure S3). The peak current with 0.5-μM flaving exhibited the highest value of 1.29 A/m², which was slightly higher than that without flavin dosing (1.18 A/m²). This suggests that the MB-modified electrode did not promote the flavin-based electron transfer. This result is inconsistent with the enhanced current using the MB-modified electrode (Figure 2a). Therefore, the above results further demonstrate that the direct contact between MB and the cells was the main mechanism for the enhanced electron transfer.
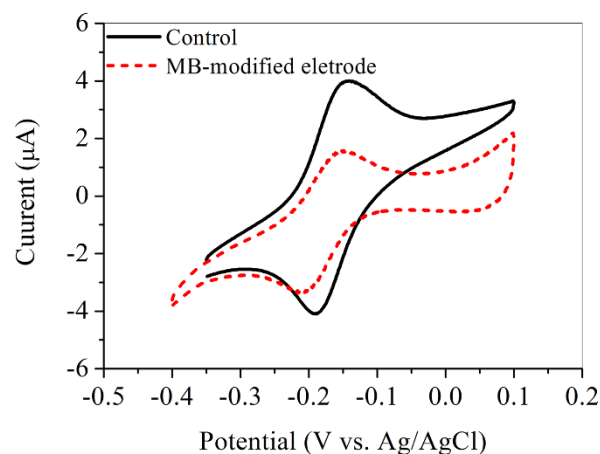
Raman spectroelectrochemical analysis on MB-mediated electron transfer. A higher net intensity of spectra was observed at a higher electrode potential (Figure 4), where MB was in its oxidized form. The number and position of the bands, as well as their relative intensities, changed substantially with the electrode potential. Obviously, the MB layer underwent redox changes with the varying electrode potentials.

Because of the complexity of this process, DFT calculations were performed to unambiguously identify the corresponding surface species. The detailed information about the calculated results is provided in the Supporting Information (SI). Strong Raman bands located within the region of 1609–1339 cm⁻¹ belong to skeleton stretch vibrations of MB in the oxidized form according to the calculated results. An intense band centered at 1620 cm⁻¹ for high electrode potentials corresponds primarily to aromatic ring stretching

Figure 3 | CV of 5-μM flavin in fresh mineral medium solution with the dose 0.1 M KCl at scanning rate of 0.05 V/s using the bactieria-free glassy carbon electrode and the MB-modified glassy carbon electrode.

scissor bending vibrations of H30-C18-H32 and H36-C20-H37 bonds, asymmetric stretches vibration of C6-N7-C8 bond, and skeleton stretch vibrations of Rings I and III (Table S2).

A shift of electrode potential to a lower value, especially lower than -0.3 V, resulted in a decrease in the intensity at 1620 cm^{-1} and 1434 cm^{-1} band length. According to the DFT calculations, the length of C6-N7, N7-C8, C5-S10, and S10-C9 bonds would increase

Figure 2 | Microbial EET at the MB-immobilized electrode with *Shewanella oneidensis* MR-1 wild type. (a) Δ*OmcA*/*MtrC* mutant (b) and Δ*MtrB* mutant (c).
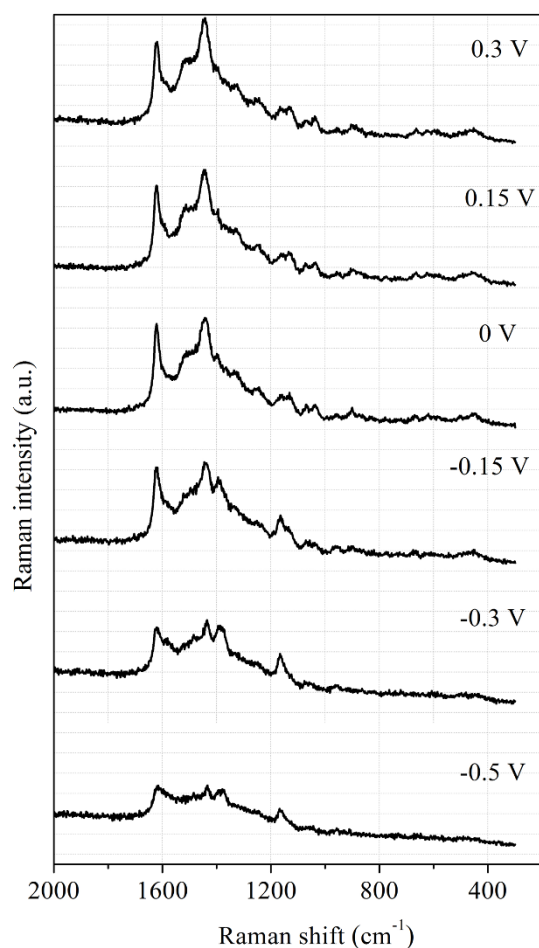
vibrations of short C3-N15, C12-N16 bonds, and aromatic ring C-C in-plane stretching vibrations coupled with scissor bending vibrations of C-H in the -CH$_3$ group. A strong band at 1444 cm^{-1}, observed for an oxidized form of MB was assigned to ring C-C stretching vibrations or asymmetric C-N stretches[22]. Calculations have shown that this mode composed primarily from bending deformation vibrations of H28-C17-H29 and H33-C19-H34 bonds,

Figure 4 | Potential-dependent Raman spectra of MB on Au electrode.

Table 1 | Geometry Parameters of Optimized Molecular Structures of MB in Its Oxidized and Reduced Forms

Bond	Length (oxidized form) (Å)	Length (reduced form) (Å)
C3-N15	1.358	1.398
C12-N16	1.358	1.399
C6-N7	1.339	1.408
N7-C8	1.339	1.408
C5-S10	1.747	1.783
S10-C9	1.747	1.783

Bond	Angle (oxidized form) (°)	Angle (reduced form) (°)
C6-N7-C8	123.171	120.983
C5-S10-C9	103.218	99.519

with a lowering potential (Table 1). This leads to the expansion of Ring II, which is responsible for a decrease in the intensity for 1620 cm^{-1} band, while the rock vibrations of C-H bonds in Rings I and III coupled with scissor bending vibrations of C-H in the -CH$_3$ group results in a decrease in intensity of 1434 cm^{-1} bond. With a decrease in potential, the intensity at 1393 cm^{-1} increased and peaked at around -0.15 V. By referring to Table S3, it could be concluded that this band is associated with rock vibrations of N7-H39 bond, and the scissor bending vibrations of C6-N7-C8 bond. Therefore, the conformation changes of MB in the redox process can be easily probed according to the relative intensity variations of these characteristic bands.

Discussion

In this work, a small-molecular-weight active phenothiazine derivative, MB, was immobilized on electrode surface to substantially enhance the microbial EET, and the interactions between the bacterial outer-membrane cytochromes and such a derivative were probed using *in situ* Raman spectro-electrochemical method coupled with DFT calculations for the first time.

Phenothiazine have multiple forms with different redox properties[23], which influenced the electron transfer capacity. In this study, we attempted to explore the functions of a series of phenothiazine derivatives in the microbial EET of *S. oneidensis* MR-1 by directly recording the current. The results clearly show that the maximum microbial current generation was closely related to the redox potentials of the phenothiazine derivatives. This is consistent with previous studies on microbial reduction of lepidocrocite and azo dyes[24]. This also implies that there is a correlation between the rate of mediated redox reactions and the reduction potential of electron transfer mediators[24,25]. With a consideration of different substrates and electron acceptors, mediators are chosen by their tunable redox potentials in the aqueous solution. Thermodynamically, substrates have their standard potential values, e.g., -0.29 V for CO$_2$/acetate, -0.19 V for pyruvate/lactate[26]. The standard potential of the mediators should be as close to that of the substrate as possible in order to obtain a maximum energy output. Thus, for a specific electron flow route, it is possible to lower the biological energy acquisition and increase the energy conversion efficiency by choosing an appropriate mediator, such as MB in this study. Generally, a bacterium needs a minimum free energy of about -20 kJ/mol to exploit the free energy change in a reaction[27]. When this thermodynamic requirement is met, phenothiazine derivatives with a lower redox potential tend to have a greater electron mediation capacity in the subsequent electron transfer process from electron shuttle to electron acceptor (i.e., electrode).

Electron transfer mediators could assist in microbial energy metabolism by facilitating electron transfer between microbes and electron-donating or accepting substances. Our study reports, for the first time, the direct interactions between *c*-type cytochromes of

electricity-generating bacteria and phenothiazine derivative molecules immobilized on a carbon electrode. The conformation shift of phenothiazine in the redox reaction process was revealed by a combined use of Raman spectroelectrochemical approach and DFT calculation. The results clearly show a distinct improvement of microbial current generation at the electrode resulted from the well communication between *c*-type cytochromes of *S. oneidensis* MR-1 and MB.

From a molecular level point of view, elucidation of the redox process of phenothiazine when it interacts with bacteria in the anode is one important fundamental challenge for the mediated electron transfer. The oxidation-reduction reaction of MB used in this study is a two-electron reaction[23]. The uptake and release of electrons lead to the changes in conformation of MB molecule. The structure variations of MB at the electrode/liquid interface probed by the *in-situ* Raman approach coupled with DFT calculation in electrochemical oxidation and reduction, reveals its role in the electron shuttling between bacteria and solid electron acceptors. In the oxidation process, two electrons are released to electrode, resulting in the shrink of active Ring II in MB molecule; when it is reduced by bacteria, MB uptakes two electrons and one proton to form a new N-H bond (Figure S4). This is responsible for the expansion of Ring II of MB (Table 1).

For *S. oneidensis* MR-1, the metal respiratory pathway (Mtr) is recognized as the most important anaerobic respiratory pathway to transfer electron from the cytoplasmic membrane to extracellular electron acceptor[28]. This pathway is also associated with the electron transfer from cell surface to MFC electrode through direct transfer by cytochromes or via indirect transfer by flavins[29]. Both *MtrC* and *OmcA* are located on the cellular outer membrane surface, and they can be directly involved in electron transfer to an extracellular solid electron acceptor, such as Fe(III) minerals[30], or to extracellular electron shuttles[12]. Δ*OmcA/MtrC* mutant is severely impaired in the sustained electron transfer, but it could attach to electrodes in a similar manner[31]. Porphyrin iron is the structure centre of *c*-type cytochromes, which play an important role in the redox process (Figure 5). Therefore, the electron transfer from *c*-type cytochromes to phenothiazine electron shuttles was reasonably substituted to the interactions between porphyrin iron and MB molecule. The proposed mechanism for the electron transfer process is illustrated in Figure 5a and b. Porphyrin iron (Fe^{2+}) as the electron donor approaches to the electron acceptor (MB oxide), and the distance between Fe^{2+} of porphyrin iron and S atom of Ring II in MB oxide is 8.147 Å, while the value in the porphyrin iron (Fe^{3+})-MB reduction system decreases to 5.175 Å. This indicates that the redox reaction occurs in the surrounding of porphyrin with the range of 5–8 Å, which is the core structure of *c*-type cytochromes.

The negative energy change ($\Delta E = -0.594$ eV) of the electron transfer (Table S4) reveals that the porphyrin iron (Fe^{3+})-MB reduction system (Figure 5b and d) is more stable than the porphyrin iron (Fe^{2+})-MB oxide system (Figure 5a and c) in the aqueous solution. Therefore, the oxidized form of the MB molecule could easily take electrons from the *c*-type cytochromes, and transfer them to electron acceptors with a higher potential.

The redox mediators excreted by *S. oneidensis* MR-1 are usually found at a level of μM or nM concentration[32]. It could accelerate electron transfer and catalyze electron transfer at a lower applied potential[31]. However, the redox peak current at the MB-modified electrode was lower than that at the control electrode (Figure 3). This implies that the direct contact between MB and the biofilm should be the main mechanism for the enhanced microbial EET at bacteria/solid electron acceptor interface.

In conclusion, the immobilized phenothiazine on solid electrode was found to enhance microbial EET in BES. The *in situ* Raman spectro-electrochemical analysis clearly demonstrates that the mediated EET process was achieved through changes in molecular
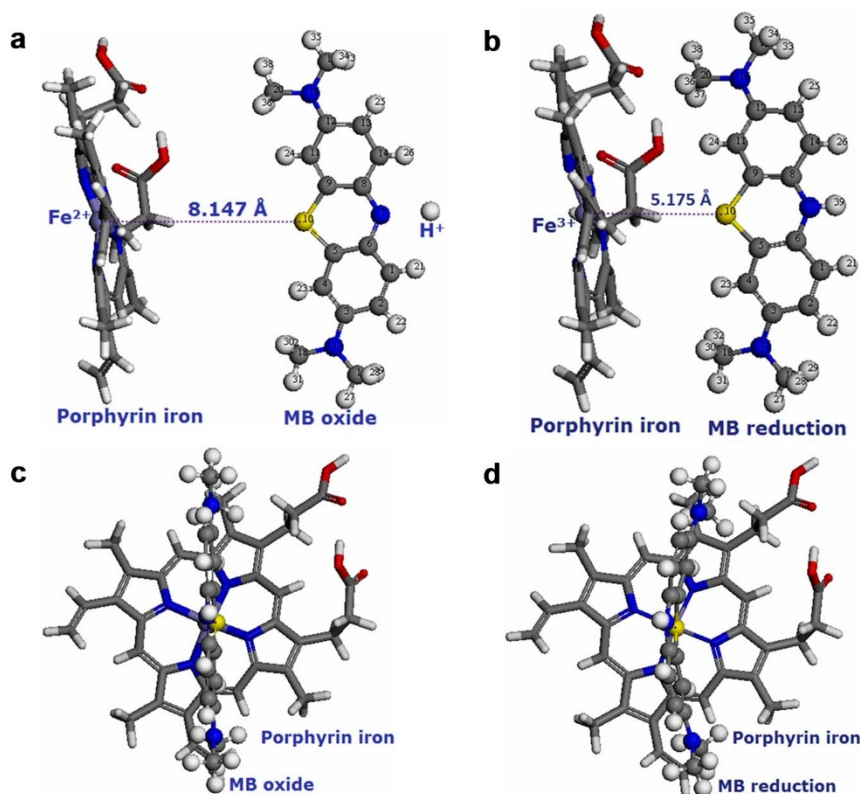
Figure 5 | Optimized molecular structures of porphyrin iron in reduced form and MB in oxidized form (a) front view and (c) side view, and porphyrin iron in oxidized form and MB in reduced form (b) front view and (d) side view: gray: carbon atom; white: hydrogen atom; blue: nitrogen atom; yellow: sulfur atom; red: oxygen atom; purple: iron atom.

conformation of phenothiazine. These findings are beneficial for designing new electrode interface to improve the current density of BES. In addition, they are also useful to better understand the microbial EET mechanism, which is crucial to develop and apply BES, biosensors or related bioelectronic devices. These findings may also have general implications in the biogeochemical cycles, biocorrosion and bioremediation.

Methods

Bacterium and cultivation. The wild type *S. oneidensis* MR-1 and its mutant strains, kindly provided by Prof. K. H. Nealson at the University of Southern California[33], were grown from a frozen stock, first aerobically in 100-ml Luria-Bertani broth, a solution of 10 g/l tryptone, 5 g/l NaCl, and 5 g/l yeast extract, at 30°C for 12 h. Subsequently, the culture of 0.5 ml was anaerobically incubated in a mineral medium (40 ml) containing (per liter) 10 mM Hepes, 0.46 g of NH_4Cl, 0.225 g of K_2HPO_4, 0.225 g of KH_2PO_4, 0.117 g of $MgSO_4 \cdot 7H_2O$, and 0.225 g of $(NH_4)_2SO_4$. Prior to autoclaving, 10 ml of a mineral mix (containing per liter 1.5 g of nitrilotriacetic acid, 0.1 g of $MnCl_2 \cdot 4H_2O$, 0.3 g of $FeSO_4 \cdot 7H_2O$, 0.17 g of $CoCl_2 \cdot 6H_2O$, 0.1 g of $ZnCl_2$, 0.04 g of $CuSO_4 \cdot 5H_2O$, 0.005 g of $AlK(SO_4)_2 \cdot 12H_2O$, 0.005 g of H_3BO_3, 0.09 g of Na_2MoO_4, 0.12 g of $NiCl_2$, 0.02 g of $NaWO_4 \cdot 2H_2O$, and 0.10 g of Na_2SeO_4) were added[31]. Medium was sparged with N_2 gas, adjusted to pH 7.2, and autoclaved.

All solutions were prepared from reagent grade chemicals without further purification. Toluidine blue O, Thionine, and MB were purchased from Aladdin Reagent Co., China.

Electropolymerization of MB. The electropolymerization of MB on carbon paper electrode (2×3 cm², 190 μm thickness, Toray Co., Japan) was carried out using cyclic voltammetry (CV) in a potential range of −1.0 to 1.2 V at a sweep rate of 0.1 V/s in Britton-Robinson (B-R) buffer solution[34] (pH 7.0) with 30 cycles (Figure S1). The MB concentration was usually 0.5 mM. After the MB film was formed on the carbon paper surface, the electrode was rinsed thoroughly with distilled water.

Three-electrode experiments. A single-chamber, three-electrode system was used, in which a Ag/AgCl (3 M KCl) and a Pt wire were used as the reference electrode and counter electrode respectively. For the selection of the phenothiazine derivatives, they were chosen according to their tunable redox potentials in the aqueous solution. Three different mediators were chosen: Toluidine blue O (redox potential, $E^0 =$

0.027 V vs. Standard Hydrogen Electrode, SHE, pH = 7.0), Thionine ($E^0 = 0.060$ V), and MB ($E^0 = 0.011$ V)[20]. The above mediator solutions were individually added to the mineral medium containing 10 mM lactate after filtration sterilization to make the final concentration of 1 μM. Carbon paper (2×3 cm², 190 μm thickness, Toray Co., Japan) was used as the working electrode.

To evaluate the enhancement of microbial EET by the immobilized MB film, carbon paper electropolymerized with MB was used as the working electrode, while raw carbon paper was used in the control tests. The freshly prepared cell suspension was inoculated into the reactor at a constant voltage of 0.1 V (vs. Ag/AgCl, 3 M KCl) held with a model CHI 1030A electrochemical workstation (Chenhua Instrument Co., China). After the working electrodes were poised at 0.1 V for at least 12 h and the biofilm was formed on the electrodes, 1 mL of concentrated lactate solution was injected to the three-electrode system to make a concentration 10 mM. Each experiment was conducted at least two times.

Electrochemical characterization. CV measurements of flavin at the MB-modified electrode were conducted using a conventional three-electrode cell with a platinum wire as the counter electrode and a Ag/AgCl (3 M KCl) as reference in a CHI 660C Electrochemical Workstation (Chenhua Instrument Co., China). MB-modified glassy carbon electrodes (3-mm diameter) were used as the working electrodes. Before use, the carbon electrodes were carefully polished to a mirror finish with 1.0, 0.3, and 0.05 μm alumina slurries successively. The electrolyte was 5 μM flavin in mineral medium solution with 0.1 M KCl added. The scanning rate was 0.05 V/s. The solution was de-aerated by passing highly pure nitrogen for 20 min before the electrochemical experiments, and a continuous flow of nitrogen was maintained over the sample solution during experiments.

Raman *in-situ* spectro-electrochemical experiments were conducted in a closed cylindrical three-electrode cell with a platinum wire counter electrode, and an Ag/AgCl reference electrode. The cell was filled with the B-R buffer solution. To obtain enhanced Raman signal, Au disc electrode (2 mm in diameter) electropolymerized with MB was used as the working electrode. Raman spectra were obtained using a LABRAM-HR Raman spectrometer with an excitation wavelength of 514.5 nm generated by an Ar^+ laser. The beam was focused to a spot of ca. 1 mm² area on the electrode surface. The experiments were carried out in 90° scattering geometry. The integration time was 10 s. In order to reduce photo- or thermo-effects and a possible degradation of MB film by the incident light, the spectroelectrochemical cell and the working electrode were periodically moved with respect to the laser beam. All potential values given are referred to Ag/AgCl reference electrode.

DFT simulations. The minimum-energy geometry structures of the oxidized and reduced methylene blue were determined by DFT computation. For the calculations, an all-electron method, which is within the Perdew-Wang 91 (PW91) form of generalized gradient approximation[35,36] for the exchange-correlation term, is used as implemented in the DMol[3] code[37,38]. This method adopts double precision numerical basis sets that take into account p polarization (DNP). The sizes of the DNP basis sets are comparable with the 6–31G** basis and are regarded as more accurate than Gaussian basis sets of the same size[39]. The DNP basis sets were used to describe the valence electrons, while all-electron core treatment was utilized to describe the core electrons. A spin-polarized scheme was used to deal with the open-shell systems. The energy in each geometry optimization cycle was converged to within 1×10^{-5} Hartree with a maximum displacement and force of 5×10^{-3} Å and 2×10^{-3} Hartree/Å, respectively. Frequency calculations were performed at the same level of theory to characterize the stationary points on the potential surface and to obtain Gibbs free energies, which were calculated at a standard pressure of 1 atm. The calculated vibrational frequencies were compared with the experimental data.

Calculations on the interactions between porphyrin iron and MB. The interactions between porphyrin iron and MB in the process of electron transfer were carried out for all structures using the GULP code[40,41]. The GULP geometry optimization is based on reducing the magnitude of calculated forces and stresses until they become smaller than defined convergence tolerances. The energy tolerance and gradient norm tolerance were smaller than 0.00001 eV and 0.001 eV/Å, respectively. The geometry structure of electron transfer systems was refined to obtain a stable structure with the minimized total energy. Then, the interaction energy of electron transfer and the distance between the active sites of porphyrin iron and MB could be analyzed. The Dreiding forcefield[42] is a purely diagonal forcefield with harmonic valence terms and a cosine-Fourier expansion torsion term. The umbrella functional form was used for inversions, which are defined according to the Wilson out-of-plane definition. The van der Waals interactions are described by the Lennard-Jones potential. Electrostatic interactions are described by atomic monopoles and a screened (distance-dependent) Coulombic term. The COSMO implementation in GULP[41] is a continuum solvation model, in which the solute molecule forms a cavity within the dielectric continuum of permittivity. The charge distribution of porphyrin iron and MB polarizes the dielectric medium. The response of the dielectric medium was described by the generation of the polarization charges on the cavity surface. In the COSMO solvation model, 'water' was selected as the electron transfer environment for the calculations.

1. Logan, B. E. & Rabaey, K. Conversion of wastes into bioelectricity and chemicals by using microbial electrochemical technologies. *Science* **337**, 686–690 (2012).
2. Rabaey, K. & Rozendal, R. A. Microbial electrosynthesis - revisiting the electrical route for microbial production. *Nature Rev. Microbiol.* **8**, 706–716 (2010).
3. Harnisch, F. & Schroder, U. From MFC to MXC: chemical and biological cathodes and their potential for microbial bioelectrochemical systems. *Chem. Soc. Rev.* **39**, 4433–4448 (2010).
4. Lu, A. *et al.* Growth of non-phototrophic microorganisms using solar energy through mineral photocatalysis. *Nat. Commun.* **3**, 768 (2012).
5. Nielsen, L. P., Risgaard-Petersen, N., Fossing, H., Christensen, P. B. & Sayama, M. Electric currents couple spatially separated biogeochemical processes in marine sediment. *Nature* **463**, 1071–1074 (2010).
6. Wu, X. *et al.* A role for microbial Palladium nanoparticles in extracellular electron transfer. *Angew. Chem. Int. Ed.* **50**, 427–430 (2011).
7. Pham, T. H., Aelterman, P. & Verstraete, W. Bioanode performance in bioelectrochemical systems: recent improvements and prospects. *Trends Biotechnol.* **27**, 168–178 (2009).
8. Qiao, Y. *et al.* Nanostructured polyaniline/titanium dioxide composite anode for microbial fuel cells. *ACS Nano* **2**, 113–119 (2007).
9. Rosenbaum, M., Zhao, F., Schroder, U. & Scholz, F. Interfacing electrocatalysis and biocatalysis with tungsten carbide: A high-performance, noble-metal-free microbial fuel cell. *Angew. Chem. Int. Ed.* **45**, 6658–6661 (2006).
10. Xie, X. *et al.* Three-dimensional carbon nanotube-textile anode for high-performance microbial fuel cells. *Nano Lett.* **11**, 291–296 (2010).
11. El-Naggar, M. Y. *et al.* Electrical transport along bacterial nanowires from Shewanella oneidensis MR-1. *Proc. Nat. Acad. Sci. U. S. A.* **107**, 18127–18131 (2010).
12. Marsili, E. *et al. Shewanella* secretes flavins that mediate extracellular electron transfer. *Proc. Nat. Acad. Sci. U. S. A.* **105**, 3968–3973 (2008).
13. Reguera, G. *et al.* Extracellular electron transfer via microbial nanowires. *Nature* **435**, 1098–1101 (2005).
14. Huang, Y.-X. *et al.* Graphene oxide nanoribbons greatly enhance extracellular electron transfer in bio-electrochemical systems. *Chem. Comm.* **47**, 5795–5797 (2011).
15. Newman, D. K. & Kolter, R. A role for excreted quinones in extracellular electron transfer. *Nature* **405**, 94–97 (2000).
16. Adachi, M., Shimomura, T., Komatsu, M., Yakuwa, H. & Miya, A. A novel mediator-polymer-modified anode for microbial fuel cells. *Chem. Comm.* 2055–2057 (2008).
17. Barsan, M. M., Pinto, E. M. & Brett, C. M. A. Methylene blue and neutral red electropolymerisation on AuQCM and on modified AuQCM electrodes: an electrochemical and gravimetric study. *Phys. Chem. Chem. Phys* **13**, 5462–5471 (2011).
18. Malinauskas, A., Niaura, G., Bloxham, S., Ruzgas, T. & Gorton, L. Electropolymerization of preadsorbed layers of some azine redox dyes on graphite. *J. Colloid Interface Sci.* **230**, 122–127 (2000).
19. Hernandez, M. E., Kappler, A. & Newman, D. K. Phenazines and other redox-active antibiotics promote microbial mineral reduction. *Appl. Environ. Microbiol.* **70**, 921–928 (2004).
20. Fultz, M. L. & Durst, R. A. Mediator compounds for the electrochemical study of biological redox systems: a compilation. *Anal. Chim. Acta* **140**, 1–18 (1982).
21. Zhao, Y. *et al.* Three-dimensional conductive nanowire networks for maximizing anode performance in microbial fuel cells. *Chem. Euro. J.* **16**, 4982–4985 (2010).
22. Mazeikiene, R., Niaura, G., Eicher-Lorka, O. & Malinauskas, A. Raman spectroelectrochemical study of Toluidine Blue, adsorbed and electropolymerized at a gold electrode. *Vib. Spectrosc.* **47**, 105–112 (2008).
23. Wang, Y. & Newman, D. K. R Redox reactions of phenazine antibiotics with ferric (hydr)oxides and molecular oxygen. *Environ. Sci. Technol.* **42**, 2380–2386 (2008).
24. O'Loughlin, E. J. Effects of electron transfer mediators on the bioreduction of Lepidocrocite (γ-FeOOH) by *Shewanella putrefaciens* CN32. *Environ. Sci. Technol.* **42**, 6876–6882 (2008).
25. Rau, J., Knackmuss, H. J. & Stolz, A. Effects of different quinoid redox mediators on the anaerobic reduction of azo dyes by bacteria. *Environ. Sci. Technol.* **36**, 1497–1504 (2002).
26. Thauer, R. K., Jungermann, K. & Decker, K. Energy conservation in chemotrophic anaerobic bacteria. *Bacteriol. Rev.* **41**, 100–180 (1977).
27. Schink, B. Energetics of syntrophic cooperation in methanogenic degradation. *Microbiol. Mol. Biol. Rev.* **61**, 262–280 (1997).
28. Shi, L., Squier, T. C., Zachara, J. M. & Fredrickson, J. K. Respiration of metal (hydr)oxides by *Shewanella* and *Geobacter*: a key role for multihaem *c*-type cytochromes. *Mol. Microbiol.* **65**, 12–20 (2007).
29. Coursolle, D., Baron, D. B., Bond, D. R. & Gralnick, J. A. The Mtr respiratory pathway is essential for reducing flavins and electrodes in *Shewanella oneidensis. J. Bacteriol.* **192**, 467–474 (2010).
30. Hartshorne, R. S. *et al.* Characterization of an electron conduit between bacteria and the extracellular environment. *Proc. Nat. Acad. Sci. U. S. A.* **106**, 22169–22174 (2009).
31. Baron, D., LaBelle, E., Coursolle, D., Gralnick, J. A. & Bond, D. R. Electrochemical measurement of electron transfer kinetics by *Shewanella oneidensis* MR-1. *J. Biol. Chem.* **284**, 28865–28873 (2009).
32. Torres, C. I. *et al.* A kinetic perspective on extracellular electron transfer by anode-respiring bacteria. *FEMS Microbiol. Rev.* **34**, 3–17 (2010).
33. Bretschger, O. *et al.* Current production and metal oxide reduction by *Shewanella oneidensis* MR-1 wild type and mutants. *Appl. Environ. Microbiol.* **73**, 7003–7012 (2007).
34. Britton, H. T. S. & Robinson, R. A. CXCVIII.-Universal buffer solutions and the dissociation constant of veronal. *J. Chem. Soc.* 1456–1462 (1931).
35. Perdew, J. P. *et al.* Atoms, molecules, solids, and surfaces: Applications of the generalized gradient approximation for exchange and correlation. *Phys. Rev. B* **46**, 6671 (1992).
36. Perdew, J. P. & Wang, Y. Accurate and simple analytic representation of the electron-gas correlation energy. *Phys. Rev. B* **45**, 13244 (1992).
37. Delley, B. An all-electron numerical method for solving the local density functional for polyatomic molecules. *J. Chem. Phys.* **92**, 508–517 (1990).
38. Delley, B. From molecules to solids with the DMol[3] approach. *J. Chem. Phys.* **113**, 7756–7764 (2000).
39. Inada, Y. & Orita, H. Efficiency of numerical basis sets for predicting the binding energies of hydrogen bonded complexes: Evidence of small basis set superposition error compared to Gaussian basis sets. *J. Comput. Chem.* **29**, 225–232 (2008).
40. Gale, J. D. GULP: A computer program for the symmetry-adapted simulation of solids. *J. Chem. Soc., Faraday Trans.* **93**, 629–637 (1997).
41. Gale, J. D. & Rohl, A. L. The General Utility Lattice Program (GULP). *Mol. Simul.* **29**, 291–341 (2003).
42. Mayo, S. L., Olafson, B. D. & Goddard, W. A. DREIDING: a generic force field for molecular simulations. *J. Phys. Chem.* **94**, 8897–8909 (1990).

Acknowledgements

Author contributions

X.W.L., X.F.S., G.P.S. and H.Q.Y. designed the experiments; J.J.C. conducted the DFT calculations and molecular dynamics simulations; X.W.L., X.F.S., Y.X.H., J.F.X., W.W.L., Y.Y.Z. and R.L. conducted the experiments; X.W.L., G.P.S., F. Z. and H.Q.Y. contributed to the planning and coordination of the project; X.W.L., G.P.S., F. Z., J.J.C. and H.Q.Y. wrote and edited the manuscript. All authors contributed to discussions about the results and the manuscript.

Additional information

Supplementary information accompanies this paper at http://www.nature.com/scientificreports

Competing financial interests: The authors declare no competing financial interests.